International Journal of Nanomedicine

Dovepress
open access to scientific and medical research

Open Access Full Text Article

ORIGINAL RESEARCH

Functionalized docetaxel-loaded lipid-based-nanosuspensions to enhance antitumor efficacy in vivo

This article was published in the following Dove Press journal:
International Journal of Nanomedicine

Xiuping Pang
Tianqi Wang
Dandan Jiang
Weiwei Mu
Bo Zhang
Na Zhang

School of Pharmaceutical Sciences, Key Laboratory of Chemical Biology (Ministry of Education), Shandong University, Jinan, Shandong Province 250012, People's Republic of China

Purpose: To further enhance the antitumor efficacy through targeted delivery, DTX loaded lipid-based-nanosuspensions (DTX-LNS) were prepared and functionalized by PEGylation or NGR modification to develop DSPE-PEG_{2000} modified DTX-LNS (P-DTX-LNS) or DSPE-PEG_{2000}-NGR modified DTX-LNS (N-DTX-LNS), respectively.

Methods: Based on our previous work, functionalized DTX-LNS including P-DTX-LNS and N-DTX-LNS were prepared using thin-film hydration, and then characterized. Release behavior, stability in vitro, cytotoxicity and cellular uptake of functionalized LNS were observed. To demonstrate tumor targeting efficiency of functionalized DTX-LNS, in vivo real-time and ex vivo imaging study were conducted. Furthermore, therapeutic efficacy in vivo was evaluated in an H22-bearing mice model.

Results: Functionalized DTX-LNS 100–110 nm in diameter were successfully prepared and exhibited good stability under various conditions. In vitro release studies demonstrated that DTX was released from functionalized DTX-LNS steadily and reached approximately 95% at 48 hrs. Functionalized DTX-LNS showed dose-dependent cytotoxicity and time-dependent internalization in human hepatocellular liver carcinoma cells (HepG2) cells. In vivo real-time and ex vivo imaging results indicated that tumor targeting efficiencies of P-DiR-LNS and N-DiR-LNS were 29.9% and 34.3%, respectively. Moreover, evaluations of in vivo antitumor efficacy indicated that functionalized DTX-LNS effectively inhibited tumor growth with low toxicity.

Conclusion: The functionalized LNS exhibited suitable particle size, nearly spherical structure, enough drug loading and great potentials for large-scale production. The results in vitro and in vivo demonstrated that functionalized LNS could realize tumor targeting and antitumor efficacy. Consequently, functionalized DTX-LNS could be expected to be used for tumor targeting therapy.

Keywords: docetaxel, lipid-based-nanosuspensions, NGR, PEG, nanocarriers

Introduction

Docetaxel (DTX) is a wide spectrum chemotherapeutic drug for treatment of various cancers.[1,2] However, due to poor water-solubility, commercial DTX injections, such as Duopafei® and Taxotere®, contain a large amount of the surfactant Tween 80 and ethanol to improve delivery, often resulting in several side effects after injection.[3,4] Thus, there is an urgent need to develop efficient drug delivery systems, which could improve dispersibility, solubility, absorption and accumulation in tumors.[5,6]

Correspondence: Na Zhang
School of Pharmaceutical Sciences, Key Laboratory of Chemical Biology (Ministry of Education), Shandong University, 44 Wenhuaxi Road, Jinan, Shandong Province 250012, People's Republic of China
Tel +86 531 8838 2015
Fax +86 531 8838 2548
Email zhangnancy9@sdu.edu.cn

submit your manuscript | www.dovepress.com
DovePress
http://doi.org/10.2147/IJN.S191341

Nanocarriers are emerging as effective drug delivery systems to enhance antitumor efficacy and reduce toxicity, particularly for hydrophobic drugs. Various nanocarriers such as liposomes, micelles, polymer–drug conjugates, nanoparticles and nanosuspensions have been widely studied.[7–12] However, only very few nanocarrier formulations have been approved by the Food and Drug Administration (FDA) for clinical cancer treatment.[13–16] Thus, it is necessary to develop nanocarriers that are easy to prepare and show good stability, to achieve further promotion and application of nanocarrier formulations.

In our previous studies, lipid-based-nanosuspensions (LNS) exhibited good stability, high drug loading and good biocompatibility, and the LNS preparation process was simple.[17–19] Most of LNS prepared in our previous studies possessed passive targeting ability to tumor tissues via the enhanced permeation and retention (EPR) effect. However, the tumor targeting efficiency of non-modified LNS was less than 10% which could be attributed to the clearance by the mononuclear phagocyte system (MPS) during blood circulation.[17–19] To further improve retention of nanocarriers in tumors, polyethylene glycol (PEG) has been widely used to modify the surface of nanocarriers to decrease MPS clearance.[20,21] Active targeting modifications have been widely applied to improve drug concentration at tumor sites. A wide variety of active targeting ligands including antibodies, peptides, aptamers and others could be grafted to the surface of nanocarriers.[13,22–25] Asparagine-glycine-arginine (NGR) peptides were among the most widely investigated active targeting ligands for tumor vasculature targeted delivery, and NGR-modified nanocarriers conferred active tumor targeting ability via CD13 receptor-mediated transcytosis.[25–28] Therefore, PEG or NGR modified LNS were proposed to improve the therapeutic effects of DTX in this study.

In this study, DTX-LNS was functionalized by DSPE-PEG_{2000} to prolong time in the blood circulation. To further improve accumulation of DTX-LNS at tumor sites, NGR was selected as the active targeting ligand. Morphology, particle size, zeta potential and in vitro release behaviors were studied. In vitro cytotoxicity and cellular uptake were tested in human hepatocellular liver carcinoma cells (HepG2). Furthermore, to demonstrate targeting efficiency of functionalized LNS, in vivo real-time and ex vivo imagings were carried out in an H22-bearing liver cancer xenograft murine model. An in vivo antitumor study was conducted to evaluate therapeutic efficacy of functionalized DTX-LNS. Finally, a preliminary safety evaluation of the nanocarriers was carried out.

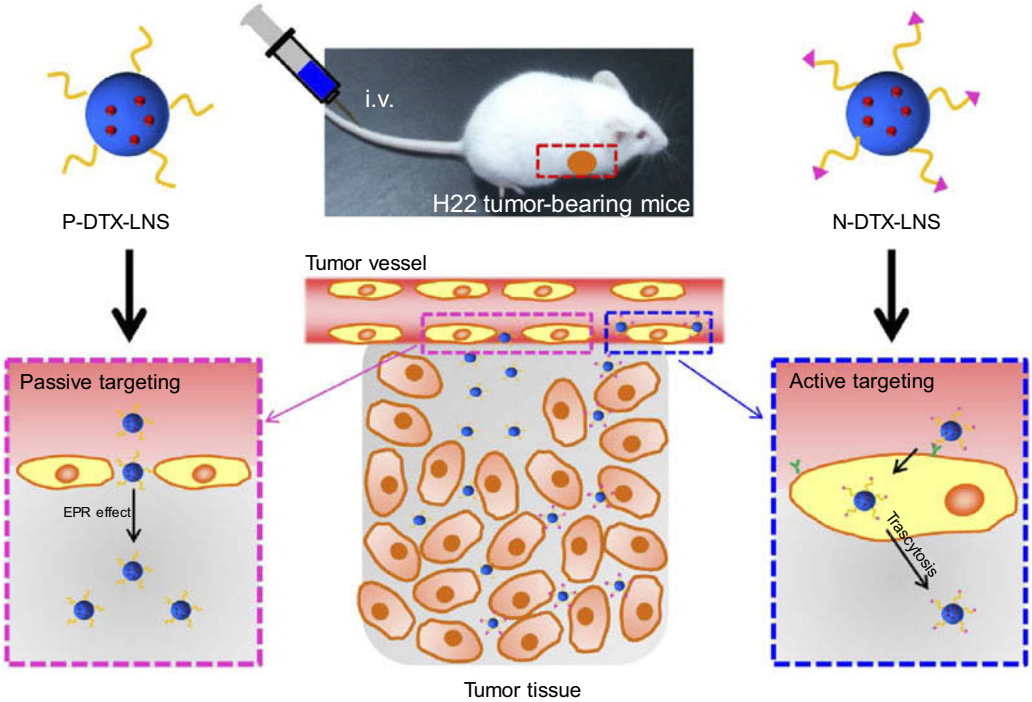

Scheme 1 (**A**) The structure representations of functionalized DTX-LNS. (**B**) The delivering mechanism of functionalized DTX-LNS. P-DTX-LNS were delivered into the tumor sites by EPR effect. Besides, N-DTX-LNS were transferred into the tumor tissue via the receptor-mediated transcytosis.
Abbreviations: EPR effect, enhanced permeation and retention effect.

Materials and methods

Materials

Docetaxel (DTX) and Duopafei® were kindly gifted by Qilu Pharmaceutical Co., Ltd. (Jinan, China). Soybean lecithin for injection was purchased from Toshisun Biology & Technology Co., Ltd. (Shanghai, China). The peptide GCNGRCGC-SH (NGR) was synthesized by Shanghai Apeptide Co., Ltd. (Shanghai, China). Coumarin 6 (CAS:38215-36-0, Aladdin) 0.1,2-distearoyl-sn-glycero-3-phosphoethanolamine-N-[methoxy(polyethyleneglycol)-2000] (DSPE-PEG_{2000}) was purchased from Avanti Polar Lipids, Inc. (Shanghai, China)0.1,2-distearoyl-sn-glycero-3-phosphoethanolamine-N-[methoxy(polyethyleneglycol)-2000]-NHS(DSPE-PEG_{2000}-NHS) was purchased from Xi'an Ruixi Biological Technology Co., Ltd.(Xi'an, China). The 1,1′-Dioctadecyl-3,3,3′,3′-tetramethylindotricarbocyanine iodide (DiR) was purchased from Fanbo Biochemicals Co., Ltd. (Beijing, People's Republic of China). All reagents for HPLC analysis were of HPLC grade. All other chemicals and reagents were of analytical grade.

Synthesis of DSPE-PEG_{2000}-NGR

The active targeting material DSPE-PEG_{2000}-NGR was synthesized by an amidation reaction between DSPE-PEG_{2000}-NHS and NGR at a 1:1 molar ratio in an ice bath for 24 hrs. Excess NGR dissolved in distilled water was added to DSPE-PEG_{2000}-NHS in dimethylformamide (DMF). Redundant NGR was removed by dialysis (MW=1,000 Da). The product was obtained after freeze-drying, and the structure was confirmed by ^{1}H-nuclear magnetic resonance (^{1}H-NMR).

Preparation of DTX-LNS, P-DTX-LNS and N-DTX-LNS

DTX-LNS was prepared using thin-film hydration. Lecithin, glycerol and DTX (10:20:1, mass ratio) were dissolved in a methanol-chloroform (2:1, V/V) mixture, dried using a rotary evaporator at 50°C, and left overnight in a vacuum desiccator. The dried film was hydrated with normal saline (NS) at 50°C, for 10 mins by ultrasound. Based on the primary formulation, DSPE-PEG_{2000} modified LNS (P-DTX-LNS, lecithin: DSPE-PEG_{2000}=95:5, molar ratio) and active targeting materials DSPE-PEG_{2000}-NGR modified LNS (N-DTX-LNS, lecithin: DSPE-PEG_{2000}: DSPE-PEG_{2000}-NGR=95:4.36:0.64, molar ratio) were prepared using the same method mentioned above.[20,22,27–30]

Characterization of DTX-LNS, P-DTX-LNS and N-DTX-LNS

Morphology was observed by transmission electron microscopy (TEM) (HT7700, Japan). Particle size and zeta potential were determined using a nano particle potential analyzer (Zeta sizer Nano ZS-90, Malvern, UK). The elements of N-DTX-LNS (5 wt% mannitol, freeze-dried) were detected by Energy Dispersive Spectrometer (Bruker Quantax 200 XFlash 6I 100, EDS). The concentration of DTX was determined by high performance liquid chromatography (HPLC) (SHIMADZULC-20AT, Japan). Drug loading efficiency (DL%) and entrapment efficacy (EE%) were calculated using the following equations:

$$\text{Drug loading efficiency (DL\%)} = W_D / W_T \times 100\% \quad (1)$$

where W_D is the weight of drug analyzed, and W_T is the total weight of drug and carrier added to the system.

$$\text{Entrapment efficacy (EE\%)} = W_D / W_{TD} \times 100\% \quad (2)$$

where W_D is the weight of drug analyzed, and W_{TD} is total weight of drug added to the system.

Stability of DTX-LNS, P-DTX-LNS and N-DTX-LNS

Physical stability was evaluated at 4±2°C,. Particle size was recorded over a period of 48 hrs. Phosphate buffer (PB 7.4 containing 0.5% Tween 80), Dulbecco's modified eagle medium (DMEM) and 10% plasma were selected for preliminary evaluation of stability at 37°C,. Particle size was also recorded for 48 hrs.

In vitro drug release study of DTX-LNS, P-DTX-LNS and N-DTX-LNS

Evaluation of in vitro release of DTX-LNS, P-DTX-LNS and N-DTX-LNS was carried out by the dynamic membrane dialysis method, and Duopafei® was selected as the control group. Phosphate buffer (PB, 0.01M, pH7.4) containing 0.5% (v/v) Tween 80 was used as the release medium. A dialysis membrane bag (MW=8,000–14,000 Da) with 2 mL of sample (100 μg/mL) was immersed in PB (15 mL) and oscillated horizontally at 37°C,. At predetermined time points, the release medium was removed and replaced with fresh buffer. The concentration of DTX was analyzed by HPLC and the cumulative release rate of DTX (CR%) was calculated using the following equation:

$$CR(\%)_n = \frac{\sum_{i=1}^{n} 17C_i}{W_o} \times 100\% \quad (3)$$

where W_0 (mg) is the primary weight of DTX in the dialysis membrane bag, and C_i (mg/mL) is the concentration of DTX in the release medium at different time points.

Cell culture

HepG2 cells (human hepatocellular carcinoma, purchased from ATCC) and H22 cells (murine hepatoma cell line, obtained from the Shandong Academy of Medical Sciences) were grown in DMEM supplemented with 10% fetal bovine serum, 100 IU/mL of penicillin and 100 μg/mL of streptomycin. HL-7702 cells (human normal liver cells, purchased from the Cell Bank of Chinese Academy of Sciences) were grown in the RPMI-1640 culture medium supplemented with 10% fetal bovine serum and 100 IU/mL of penicillin and 100 μg/mL of streptomycin. All of cell lines were maintained in a 5% CO_2 incubator at 37°C,.

In vitro cytotoxicity study

Cytotoxicity was examined in HepG2 cells using MTT assay. The cells were seeded at 5×10^3 cells/well in 96 well plates and incubated overnight at 37°C,. The cells were treated with different concentrations of LNS for 48 hrs. At the end of the incubation period, 20 μL of MTT (5 mg/mL) were added to each well. The plates were incubated for an additional 4 hrs. Dimethyl sulfoxide (DMSO) (150 μL) was added to dissolve the formazan crystals, and absorbance value was determined at 570 nm. Cell viability was calculated according to the following formula:

$$\text{Cell viability}(\%) = \frac{Abs_{sample} - Abs_{blank}}{Abs_{control} - Abs_{blank}} \times 100\% \quad (4)$$

where Abs (control), Abs (sample), Abs (blank) represented the absorbance at 570 nm of the control, sample, blank, respectively.

In vitro cellular uptake

Coumarin 6 (C6) was selected as the fluorescent dye to label the LNS. C6-LNS, P-C6-LNS and N-C6-LNS were prepared via the same method as above. HepG2 and HL-7702 cells were seeded at a density of 1.5×10^5 cells/well onto 12-well plates and incubated overnight at 37°C. Free C6, C6-LNS, P-C6-LNS and N-C6-LNS (the concentration of C6 was 200 ng/mL) were added and incubated with cells for 1 or 4 hrs at 37°C. After incubation, the cells were washed with cold PBS and the cell nuclei were stained with DAPI (2-(4-amidinophenyl)-6-indolecarbamidine dihydrochloride) during a 15 mins incubation following standard protocols. Then the cells were imaged by fluorescence microscopy (BX40; Olympus Corporation, Tokyo, Japan). To quantify cellular uptake, the cells were trypsinized, centrifuged and resuspended in 400 μL of PBS, followed by fluorescence intensity detection using flow cytometry (BD, FACS Aria III, USA).

In vivo studies

Animals

All experiments were carried out in compliance with the Animal Management Rules of the Ministry of Health of the People's Republic of China (document number 55, 2001) and the Animal Experiment Ethics Review of Shandong University (Approval No. 18002). Male Kunming mice (weight: 18–22 g, age: 6–8 weeks) were supplied by the Medical Animal Test Center of Shandong University (Jinan, China).

Establishment of tumor-bearing mouse model

H22 cells were resuscitated in 37°C, water bath and subsequently injected into the abdominal cavity of the Kunming mice. After one week, ascites was collected and diluted to 2×10^7 cells/mL. For establishment of H22 hepatocellular carcinoma, 2×10^6 H22 tumor cells (0.1 mL/mouse) were injected subcutaneously into the right flank spaces of the mice.

In vivo real-time and ex vivo imaging study

The tumor-bearing mouse model was established as described above. When the tumors grew to approximately 100 mm^3, the mice were randomly divided into 4 groups (three mice in each group) and given intravenous (iv.) injections of free DiR, DiR-LNS, P-DiR-LNS and N-DiR-LNS at a dose of 50 μg/kg. After 1, 2, 4, 8, 12 and 24 hrs post-injection, mice were anesthetized with 10% chloral hydrate (intraperitoneally [ip.]) and then placed on their back in a light-tight chamber. 24 hrs tail vein injection, the mice were sacrificed. Tumors and major organs were excised, washed and subjected to near-infrared fluorescence signal intensity measurement. Images were observed using the in vivo real-time fluorescence imaging system spectrum (Caliper PerkinElmer, MA, USA) at the appropriate wavelengths (excitation wavelength of 745 nm, emission wavelength of 835 nm). Tumor targeting efficiency was calculated according to the following formula:

$$\text{Tumor targeting efficiency } (\%) = FI_{tumor}/(FI_{heart} + FI_{liver} + FI_{spleen} + FI_{lung} + FI_{kidney} + FI_{tumor}) * 100\% \quad (5)$$

where FI was the fluorescence intensity of heart, liver, spleen, lung, kidney and tumor, respectively.

In vivo antitumorefficacy evaluation

The tumor-bearing mouse model was established as described above. When the tumors grew to approximately 100 mm^3, the mice were randomly divided into 5 groups (five mice in each group) and given intravenous (iv.) injections of normal saline (NS), Duopafei®, DTX-LNS, P-DTX-LNS and N-DTX-LNS at a dose of 5 mg/kg every two days for three weeks. Body weights and tumor volumes were recorded every other day. Tumor volumes were measured using a vernier caliper every other day by using the formula: (length × $width^2$)/2,[31] where length was the longest dimension and width was the widest dimension. At day 21, the mice were sacrificed, and the tumors were excised and weighed.

Histopathological study

To study the safety of the formulations, a histopathological study (tissue toxicity study) was carried out. In brief, major organs (heart, liver, spleen, lung and kidney) of mice that were given intravenous of NS, DTX-LNS, P-DTX-LNS and N-DTX-LNS seven times were fixed in 4% PBS buffered paraformaldehyde and embedded in paraffin wax. The paraffin-embedded 5-mm sections were stained with hematoxylin and eosin to assess histology.

Statistical analysis

The data were presented as the mean ± standard deviation (SD). One-way ANOVA was used to determine statistical significance between two groups and differences were considered to be statistically significant when the *p*-value was less than 0.05.

Results and discussion

Results

Synthesis and characterization of DSPE-PEG_{2000}-NGR

To prepare N-DTX-LNS, the active targeting material DSPE-PEG_{2000}-NGR was synthesized by an amidation reaction (Figure 1A). The ^1H NMR spectra of DSPE-PEG_{2000}-NHS, NGR and DSPE-PEG_{2000}-NGR were shown in Figure 1B. The signals at approximately 2.8 ppm were presented in DSPE-PEG_{2000}-NGR, which was attributed to methylene groups close to the sulfur atom in NGR. As a result, NGR was successfully connected with DSPE-PEG_{2000}-NHS and the NGR-modification rate was around 5%. The active targeting material DSPE-PEG_{2000}-NGR was used in the following experiments.

Characterizations

DTX-LNS, P-DTX-LNS and N-DTX-LNS were prepared by thin-film hydration. The results in Figure 2A and Table 1 show that the particle sizes of DTX-LNS, P-DTX-LNS and N-DTX-LNS were about 100 nm and zeta potential was around –2.3 mV. The DL (%) and EE (%) was high. TEM images of LNS were shown in Figure 2B, and LNS were nearly spherical particles and PEG shell of P-DTX-LNS and N-DTX-LNS could be clearly observed, which was in good agreement with the results according to the references.[32] The elements of N-DTX-LNS were detected by EDS due to that sulfur (S) was the specific element in NGR. The results (Figure 2C) indicated that there existed the signal of elemental sulfur (S) in N-DTX-LNS, which demonstrated that NGR has been successfully modified on the surface of DTX-LNS.

Stability of DTX-LNS, P-DTX-LNS and N-DTX-LNS

Stability of DTX-LNS, P-DTX-LNS and N-DTX-LNS was studied by determination of particle size alteration under different conditions. As shown in Figure 3A, the particle size of three formulations has been kept in 100–150 nm range at different conditions. These results suggested that DTX-LNS, P-DTX-LNS and N-DTX-LNS could be stored at 4±2°C, for 2 days and were stable in the PB 7.4 containing 0.5% Tween 80, DMEM and 10% plasma.

In vitro drug release study

Accumulation release of DTX in different formulations was shown in Figure 3B. Approximately 100% of DTX in Duopafei® was released within 24 hrs. However, the accumulation release of DTX in functionalized LNS reached to 95% within 48 hrs. Release behaviors of DTX in both DTX-LNS and functionalized DTX-LNS were similar, which indicated that DSPE-PEG_{2000} and DSPE-PEG_{2000}-NGR did not affect the release profiles of DTX from LNS.

In vitro cytotoxicity study

Cytotoxicity of blank LNS, free DTX, DTX-LNS, P-DTX-LNS and N-DTX-LNS was evaluated in HepG2 cells by MTT assay. As shown in Figure 4, cell viability was around 100% in the blank LNS group. It could be clearly found that the cell viability (%) decreased with the increase of DTX concentrations for functionalized DTX-LNS (five concentrations of one solution/suspension analyzed by one-way

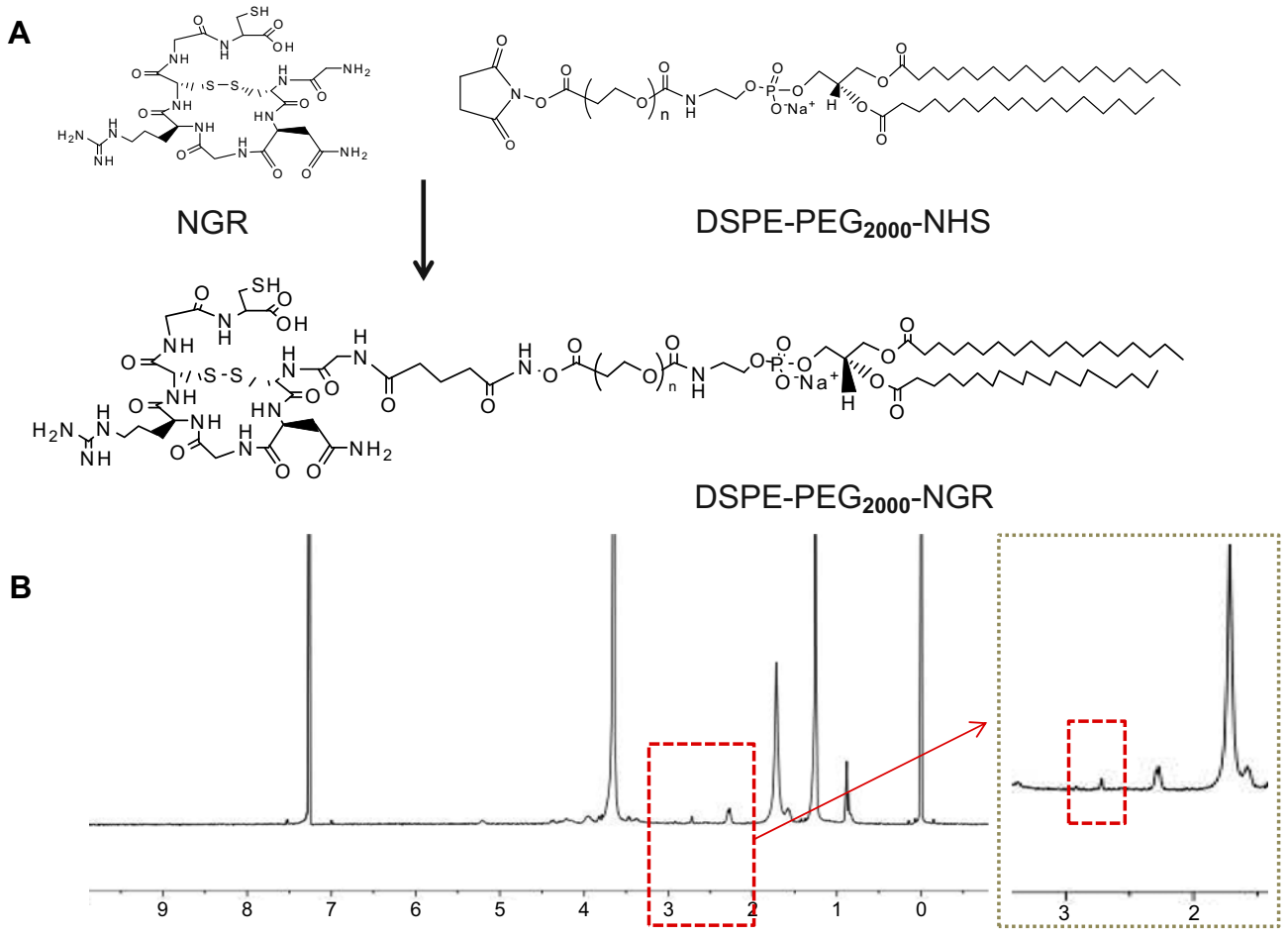

Figure 1 Synthesis and characterization of DSPE-PEG_{2000}-NGR. (**A**) The synthesis of DSPE. PEG_{2000}-NGR. (**B**) The ^{1}H NMR spectra of DSPE-PEG_{2000}-NGR.
Abbreviation: NMR, nuclear magnetic resonance.

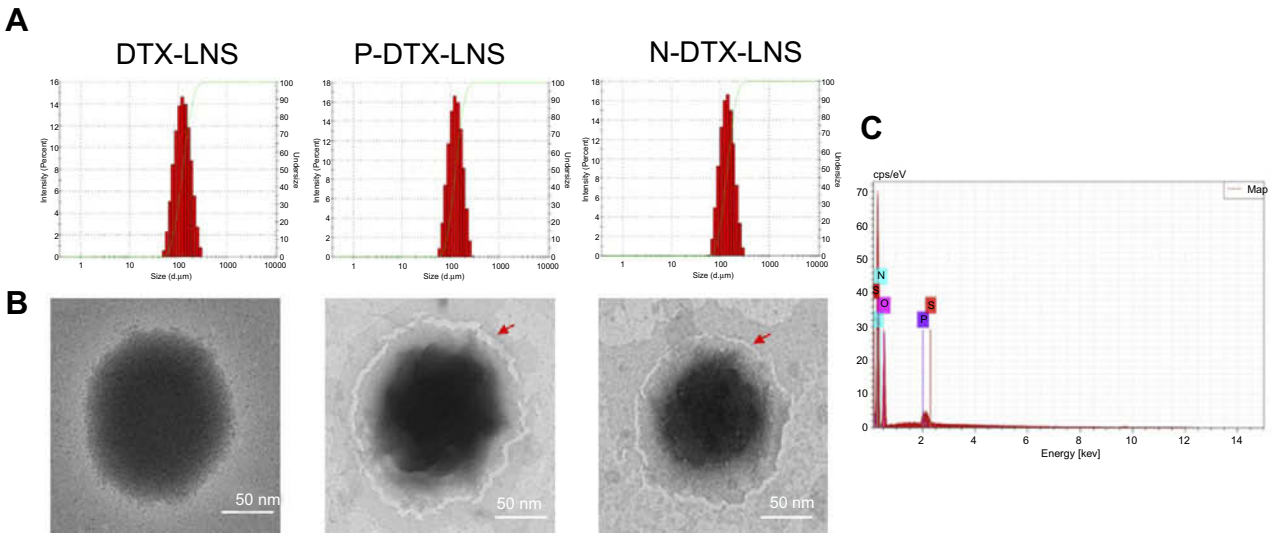

Figure 2 Characterizations. (**A**) Particle size and size distribution. (**B**) TEM images. (**C**) Energy Dispersive Spectrometer (EDS) map of N-DTX-LNS.
Abbreviation: TEM, transmission electron microscopy.

Table 1 Characterization of LNS formulations (n=3)

Formulations	DTX-LNS		P-DTX-LNS		N-DTX-LNS	
	Mean	SD	Mean	SD	Mean	SD
Size (nm)	108.43	7.46	107.15	7.12	109.43	5.13
PDI	0.340	0.057	0.302	0.012	0.277	0.018
Zeta potential (mV)	−2.24	0.184	−2.34	0.313	−2.39	0.378
Drug loading (%)	9.63	0.64	7.35	0.30	8.22	0.012
Entrapment efficacy (%)	96.86	12.17	95.62	8.01	93.96	8.12

Note: SD referred to the standard deviation of three results.
Abbreviations: nm, nanometer; PDI, polydispersity index; mV, millivolt.

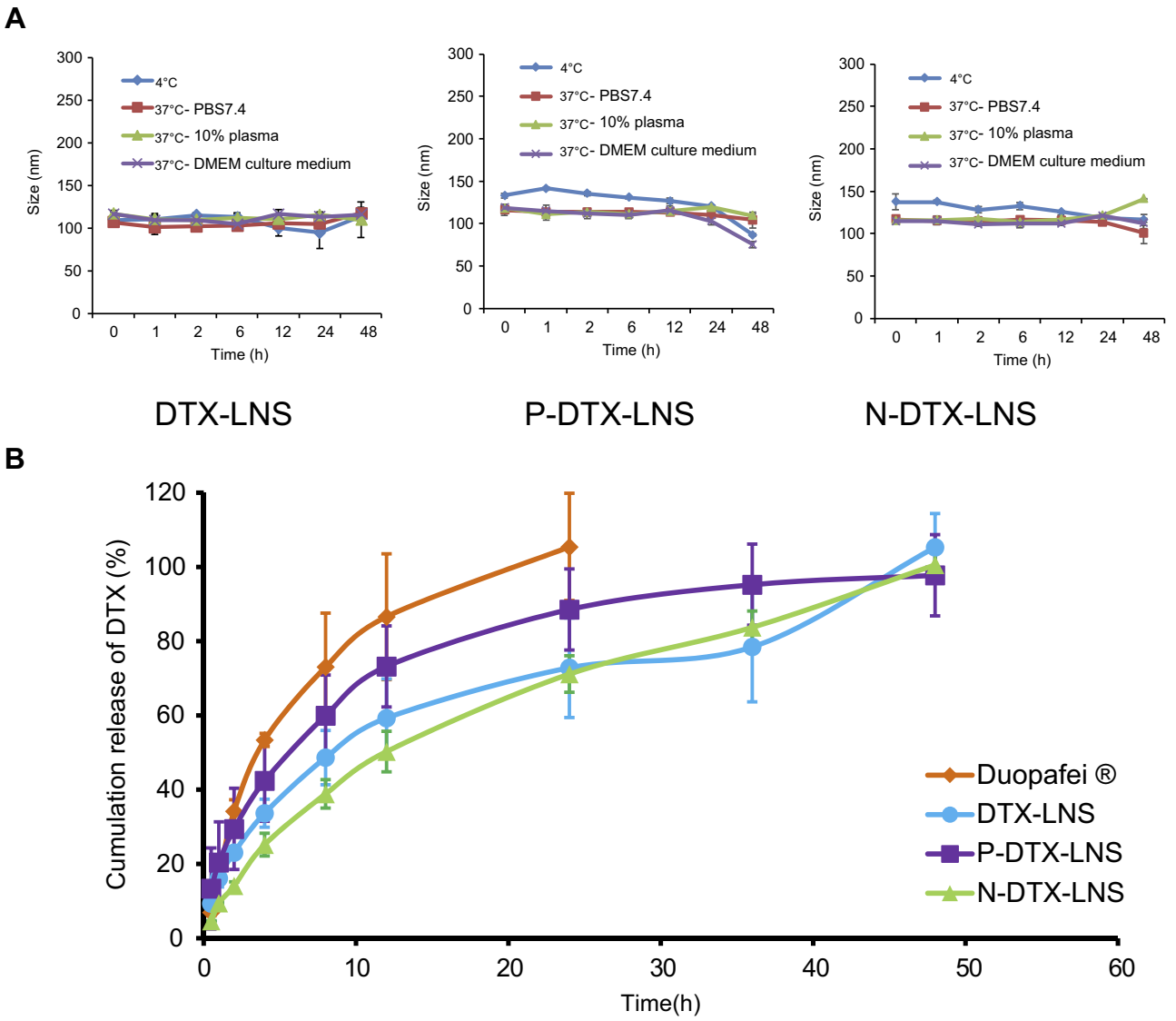

Figure 3 In vitro stability and drug release study (n=3). (**A**) Particle size changes of DTX-LNS, P-DTX-LNS and N-DTX-LNS at different conditions. (**B**) In vitro release of DTX from LNS. Data were given as mean ± SD (n=3).
Abbreviation: SD, standard deviation.

ANOVA). Thus, functionalized DTX-LNS could exhibit a dose-dependent cytotoxicity. There were no significant differences in half maximal inhibitory concentration (IC_{50}) values between functionalized DTX-LNS and

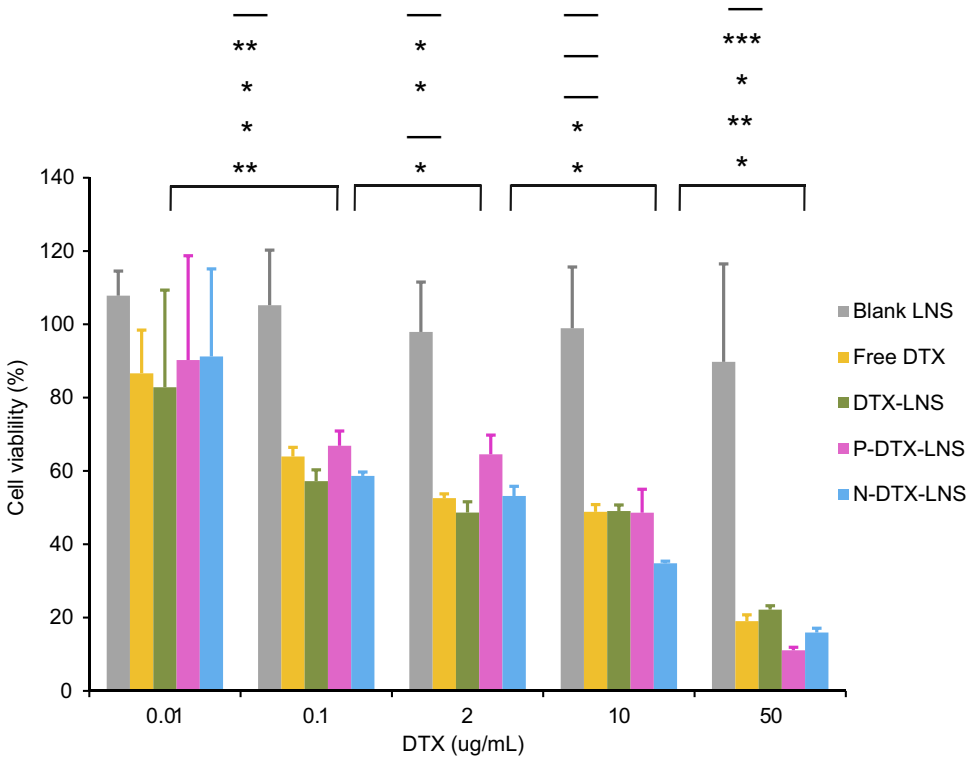

Figure 4 In vitro cytotoxicity of various concentrations of blank LNS, free DTX, DTX-LNS, P-DTX-LNS and N-DTX-LNS in HepG2 cells at 48 hrs (n=3). Data were given as mean ± SD (n=3), *p<0.05, **p< 0.01, ***p<0.001 (From top to bottom indicated the differences of blank LNS, free DTX, DTX-LNS, P-DTX-LNS and N-DTX-LNS, "-" represented that there was no significant difference).
Abbreviation: HepG2 cells, human hepatocellular liver carcinoma cells.

Table 2 IC_{50} of different DTX formulations (n=3)

Formulations	Free DTX		DTX-LNS		P-DTX-LNS		N-DTX-LNS	
	Mean	SD	Mean	SD	Mean	SD	Mean	SD
IC_{50}(μg/mL)	1.57	0.40	1.32	0.15	1.48	0.16	1.47	0.15

Note: SD referred to the standard deviation of three results.
Abbreviations: IC_{50}, half maximal inhibitory concentration; SD, standard deviation.

DTX-LNS (Table 2), which indicated that functionalized modifications on LNS did not affect cytotoxicity of DTX in vitro.

In vitro cellular uptake

To investigate uptake ability of free C6, C6-LNS, P-C6-LNS and N-C6-LNS, in vitro cellular uptake studies were conducted in HepG2 cells after 1 or 4 hrs of incubation. To further characterize the tumor-targeting ability of LNS prepared in this study, human normal liver cells HL-7702 was performed simultaneously. As depicted in Figure 5, the internalization of C6-LNS was higher than that of P-C6-LNS and N-C6-LNS after 1 hr incubation in HepG2 cells (***p<0.001 for P-C6-LNS and **p<0.01 for N-C6-LNS, respectively). However, internalization of all groups in HL-7702 cells was fewer than that in HepG2 cells at 4 hrs incubation (***p<0.001 for Free C6, *p<0.05 for C6-LNS, **p<0.01 for P-C6-LNS and ***p<0.001 for N-C6-LNS, respectively). Fluorescence microscopy images were consistent with flow cytometry analysis results.

In vivo real-time and ex vivo imaging study

In vivo real-time biodistribution and tumor-targeting ability of free DiR, DiR-LNS, P-DiR-LNS and N-DiR-LNS were observed in H22 tumor-bearing mice following intravenous injection (as shown in Figure 6). As shown in Figure 6A, the signal of free DiR group was nearly invisible in the tumor area. However, the tumor fluorescent signals of the LNS

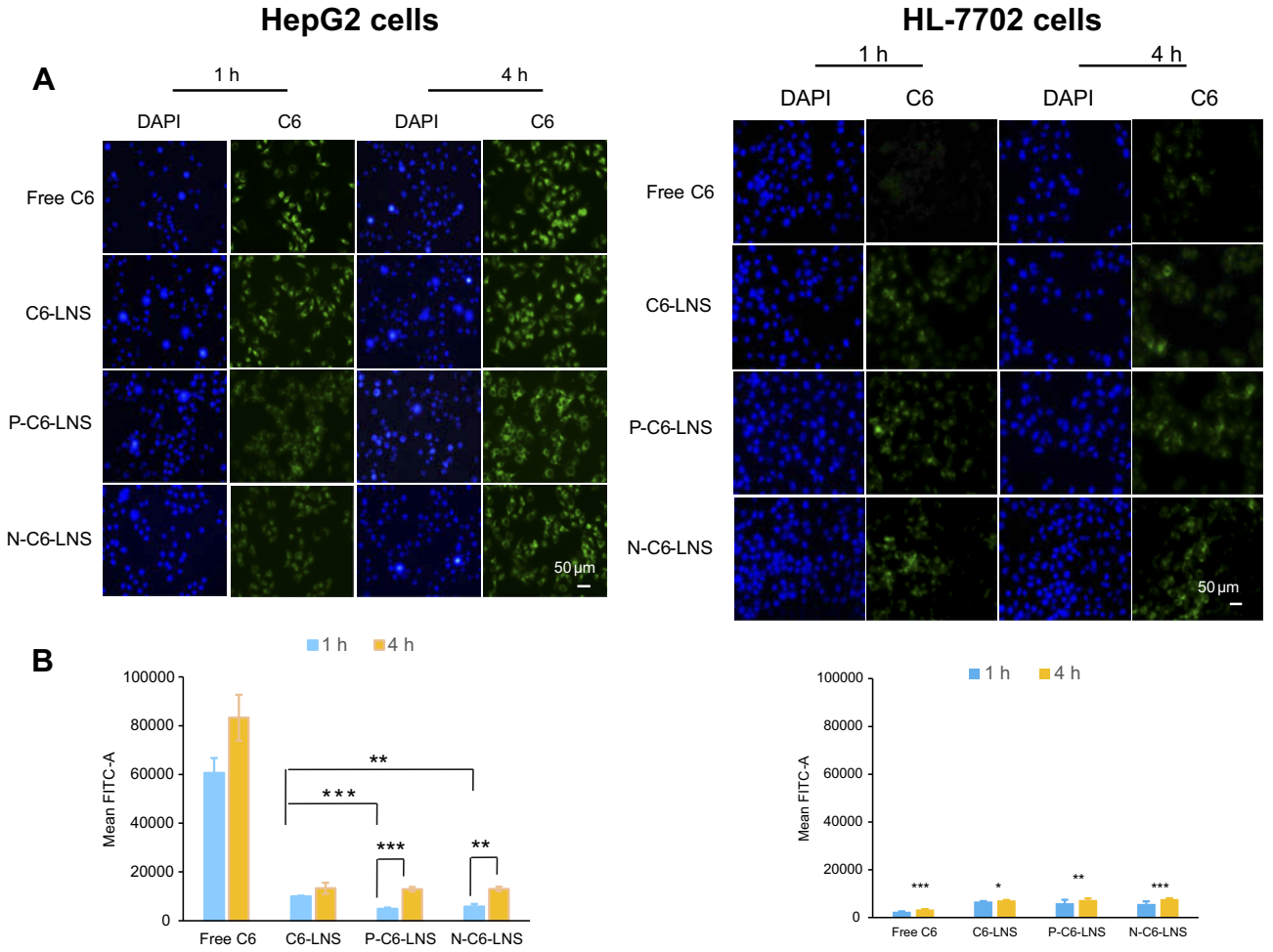

Figure 5 (**A**) Fluorescence microscopy images of HepG2 cells and HL-7702 cells after incubation with various formulations of coumarin-6 (C6) for 1 or 4 hrs including free C6 (Lane 1), C6-LNS (Lane 2), P-C6-LNS (Lane 3) and N-C6-LNS (Lane 4), for which blue and green represent the fluorescence of DAPI and C6 (bar represents 50 μm). (**B**) Internalization rates of the free C6, C6-LNS, P-C6-LNS and N-C6-LNS analyzed by flow cytometry. Data were given as mean ± SD (n= 3), *p<0.05, **p<0.01, ***p<0.001.
Abbreviations: C6, coumarin-6; DAPI, 2-(4-amidinophenyl)-6-indolecarbamidine dihydrochloride.

groups could be easily discerned 2 hrs post-injection. In addition, the signal intensity of LNS groups at the tumor site was still very strong 24 hrs after injection. Ex vivo data illustrated that dye accumulation in tumors was elevated by various modifications. In addition, tumor targeting efficiency was calculated at 24 hrs (Figure 6C), and nearly 12.9% of DiR-LNS accumulated in tumors, while the percentages of P-DiR-LNS and N-DiR-LNS that accumulated in tumors were 29.9% and 34.3%, respectively.

In vivo antitumor efficacy evaluation

Antitumor efficacy of different formulations was evaluated in H22 tumor-bearing mice. As shown in Figure 7A and B, the tumor volumes in the DTX-LNS, P-DTX-LNS and N-DTX-LNS were smaller than in those of the free DTX group (each LNS group compared with free DTX group, **p<0.01). Furthermore, tumor weight in the functionalized DTX-LNS group were smaller than those in the DTX-LNS groups (Figure 7C). Thus, functionalized modifications on DTX-LNS could improve antitumor efficacy in vivo. Compared with the body weight of NS group, the functionalized DTX-LNS group showed no changes; however, Duopafei® group decreased significantly (Figure 7D).

Histological assays

To assess the safety in vivo following treatment, hematoxylin and eosin staining of sections of major organs including heart, liver, spleen, lung and kidney was performed at day 21 in mice treated seven times with various drug formulations after injection (Figure 8). The organs of DTX-LNS, P-DTX-LNS and N-DTX-LNS groups exhibited normal histological structures.

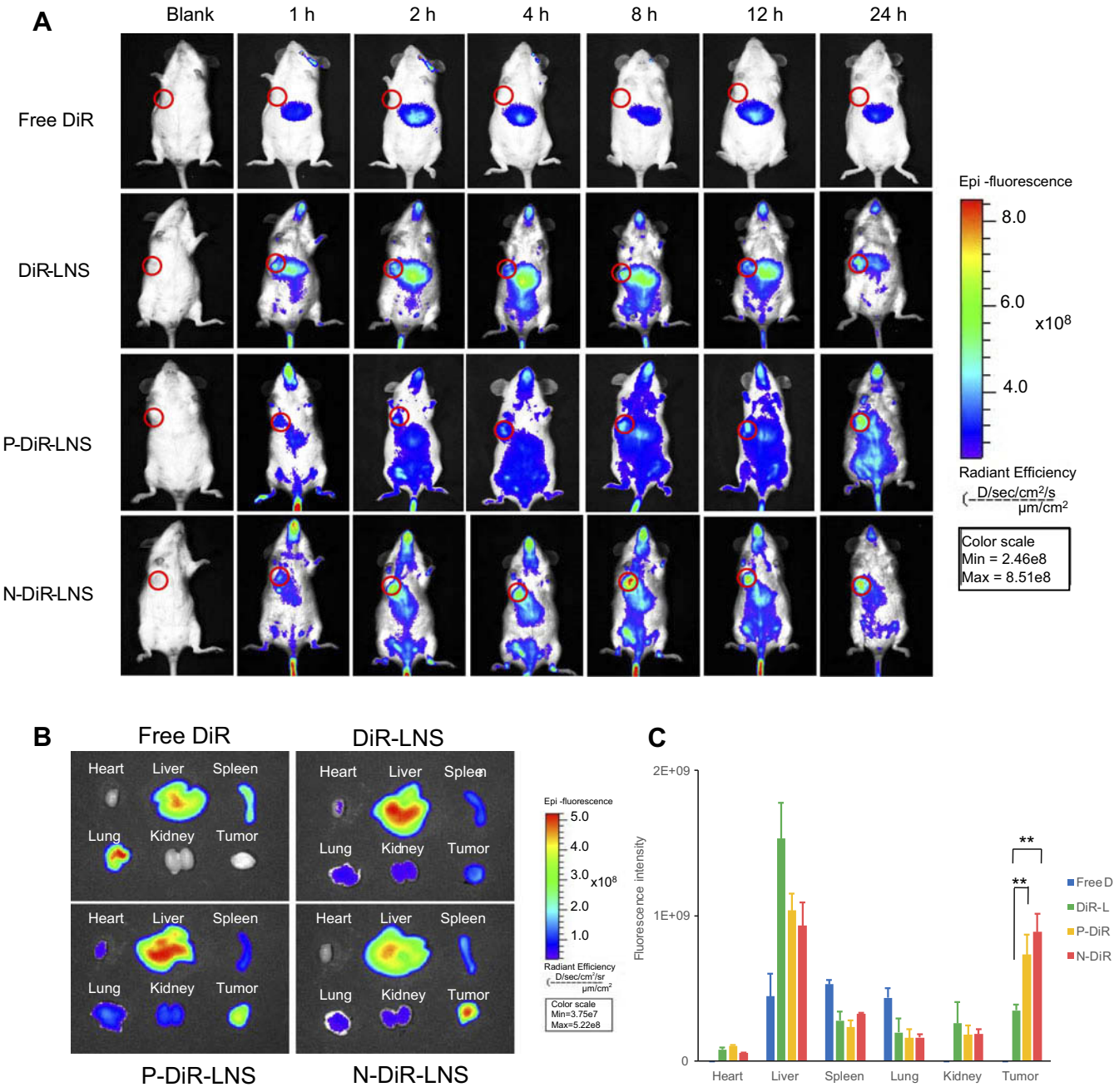

Figure 6 In vivo real-time and ex vivo imaging study of H22 tumor-bearing mice after intravenous injection of free DiR, DiR-LNS, P-DiR-LNS and N-DTX-LNS. (**A**) In vivo imaging of the mice at different time intervals; (**B**) The ex vivo images of heart, liver, spleen, lung, kidney and tumor after 24-hrs iv. injection after the mice were dissected at 24 hrs post administration; (**C**) Fluorescent intensity based on the ex vivo results. Data were given as mean ± SD (n=3), $^{**}p<0.01$.
Abbreviations: DiR, 1,1′-Dioctadecyl-3,3,3′,3′-tetramethylindotricarbocyanine iodide; IVIS, in vivo real-time fluorescence imaging system.

Discussion

Docetaxel (DTX) is a kind of hydrophobic drug, and the applications of commercial DTX injections are often limited due to the use of a large amount of the surfactant.[1–3] Nanocarriers are emerging as effective drug delivery systems for hydrophobic drugs to improve dispersibility, solubility, absorption and accumulation in tumors.[7–12] Functionalized DTX loaded lipid-based-nanosuspensions (DTX-LNS) were successfully prepared by thin-film hydration in this study and possessed the following advantages. The preparation process was simple; thus, large-scale production would be expected. The excipients in the LNS formulations including soybean lecithin, DSPE-PEG_{2000} and NGR, were biocompatible and safe,

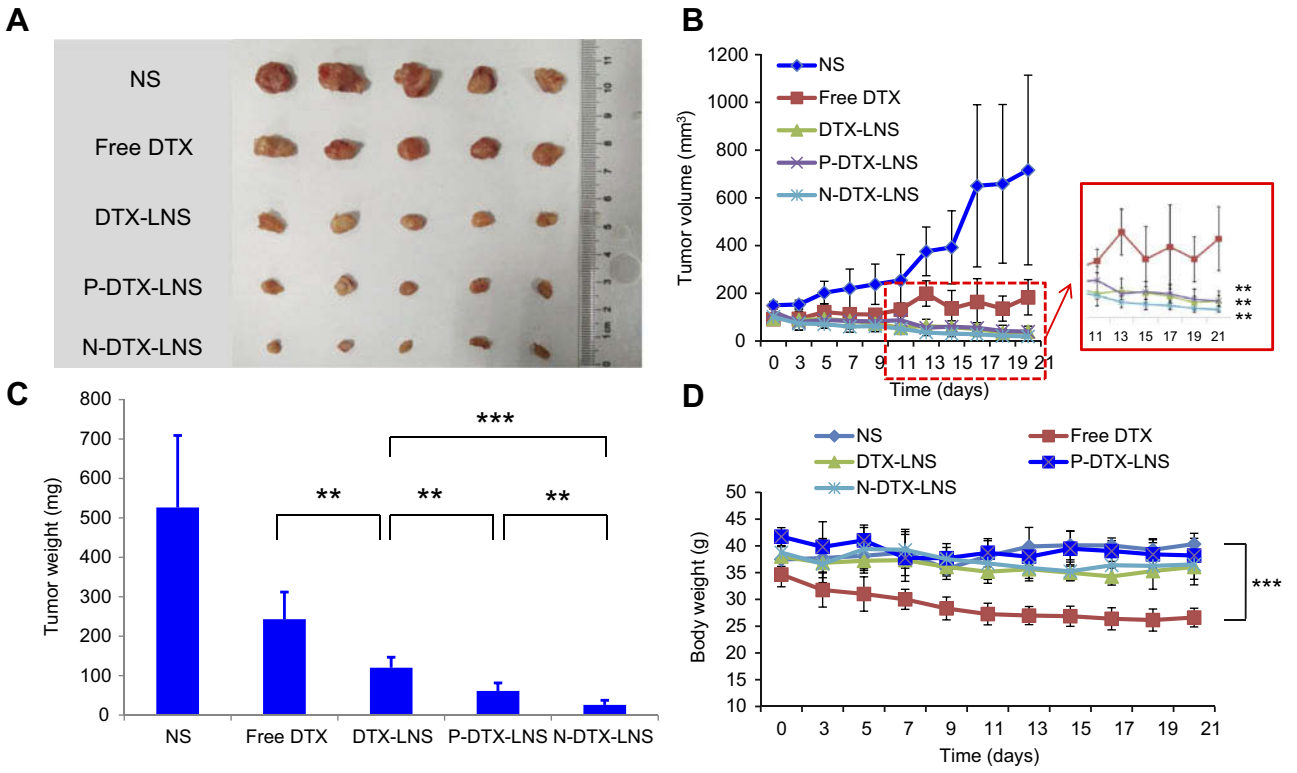

Figure 7 In vivo antitumor efficacy of NS groups, free DTX, DTX-LNS, P-DTX-LNS and N-DTX-LNS on H22 tumor-bearing mice. (**A**) Photographs of tumors excised from each treatment group on day 21; (**B**) Variation of tumor volume; (**C**) Variation of tumor weight; (**D**) Body weight change of each treatment group. Data were given as mean ± SD (n=5), $^{**}p<0.01$, $^{***}p<0.001$.
Abbreviation: NS, normal saline.

which were beneficial to reduce side effects.[33–35] The drug loading was enough to ensure the therapeutic efficacy. The results of stability study informed that the formulations of the functionalized DTX-LNS were applicable for the further clinical use.

To evaluate the tumor targeting ability of functionalized DTX-LNS, a series of experiments including in vitro and in vivo were conducted. Cellular uptake experiments in human hepatocellular carcinoma HepG2 cells and human normal liver cells HL-7702 cells were studied simultaneously and the internalization of functionalized C6-LNS in HepG2 cells was significantly higher than that in HL-7702 cells after 4 hrs of incubation ($^{***}p<0.001$ for Free C6, $^{*}p<0.05$ for C6-LNS, $^{**}p<0.01$ for P-C6-LNS and $^{***}p<0.001$ for N-C6-LNS, respectively). Moreover, in vivo real-time and ex vivo imaging study was further carried out and the tumor targeting efficiency at 24 hrs of P-DiR-LNS or N-DiR-LNS was significantly higher than that of unfunctionalized DiR-LNS ($^{**}p<0.01$). Although it was just a preliminary evaluation and cannot entirely substitute for real drug biodistribution due to the differences between fluorescent dye and drug, it indicated the tumor accumulation capacity to a certain extent. These results demonstrated that functionalized LNS prepared in this study possess preferable tumor targeting ability.

The antitumor efficacy of functionalized DTX-LNS was also investigated both in vitro and in vivo. There were no significant differences in the in vitro cytotoxicity between functionalized DTX-LNS and unfunctionalized DTX-LNS, which indicated that functionalized modifications on LNS did not affect cytotoxicity of DTX in vitro. The functionalized DTX-LNS including P-DTX-LNS or N-DTX-LNS exhibited significantly superior antitumor efficacy in vivo compared with unfunctionalized DTX-LNS ($^{**}p<0.01$ for P-DTX-LNS and $^{***}p<0.001$ for N- DTX-LNS in Figure7C, respectively). It could be attributed that the PEG shell of P-DTX-LNS and N-DTX-LNS were beneficial for circulation stability in vivo and NGR modification could further improve the tumor targeting ability of N-DTX-LNS.

Over all, functionalized DTX-LNS prepared in this study would be the desired carrier for hydrophobic DTX delivery and possess great potentials for clinical application.

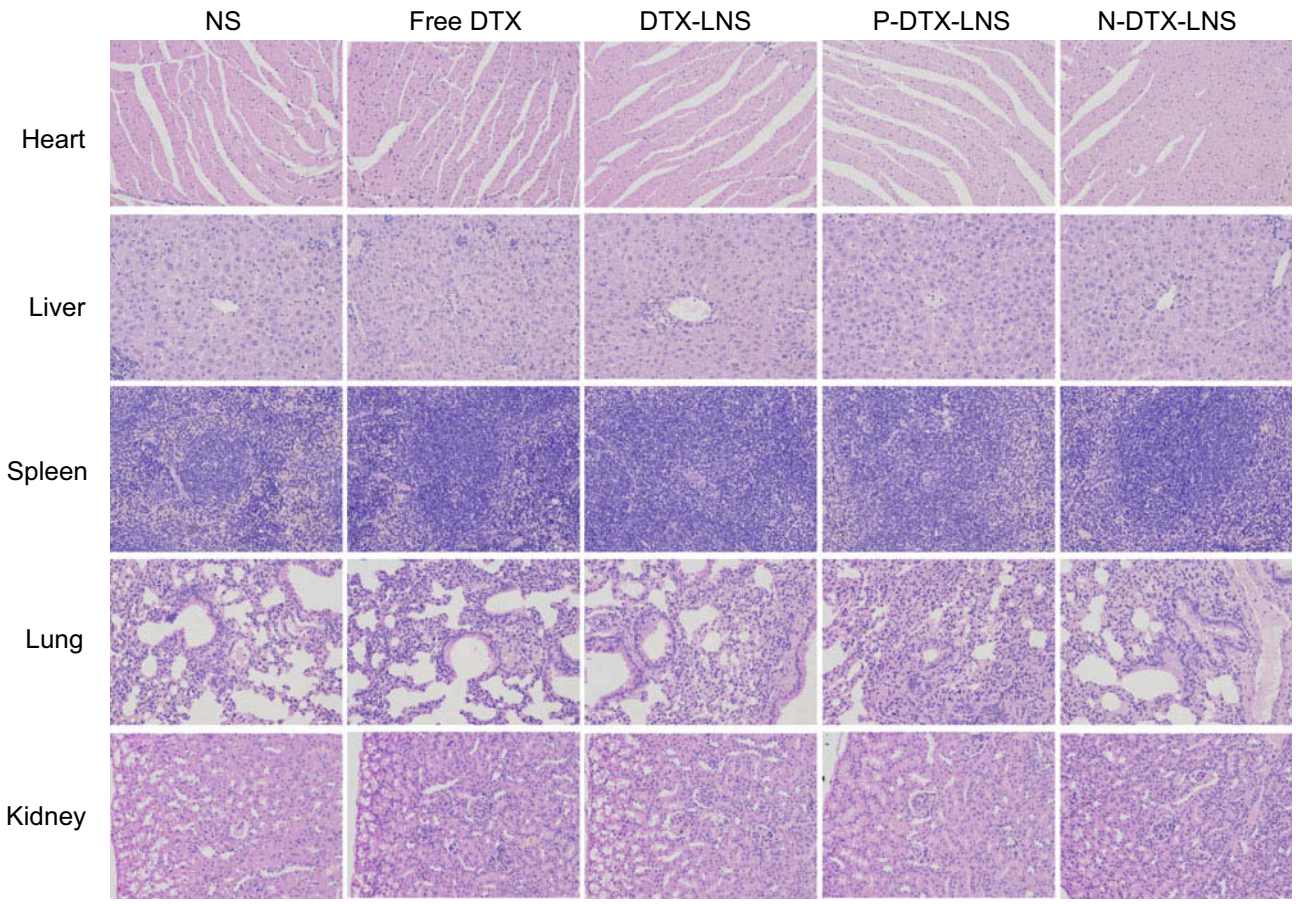

Figure 8 Histological assays (Representative microscopy images of H&E-stained histological sections after treatment with NS groups, free DTX, DTX-LNS, P-DTX-LNS and N-DTX-LNS). Magnification 200×.
Abbreviations: NS, normal saline; H&E, hematoxylin and eosin.

Conclusion

In the present study, we successfully prepared two kinds of functionalized LNS including P-DTX-LNS and N-DTX-LNS. The functionalized LNS exhibited suitable particle size, nearly spherical structure, enough drug loading and great potentials for large-scale production. The results in vitro and in vivo demonstrated that functionalized LNS could realize tumor targeting and antitumor efficacy. Consequently, functionalized DTX-LNS could be expected to be used for tumor targeting therapy.

Acknowledgment

This work was supported by the National Natural Science Foundation of China (grant number: 81573368).

Disclosure

The authors report no conflicts of interest in this work.

References

1. Keskin SK, Yildirim A, Canakci C, et al. The use of PSA doubling time to predict prognosis and the use of PSA response to assess the success for prostate cancer patients undergoing docetaxel chemotherapy. *J Cancer Ther*. 2016;07(08):593–599. doi:10.4236/jct.2016.78062
2. Borghaei H, Paz-Ares L, Horn L, et al. Nivolumab versus docetaxel in advanced nonsquamous non–small-cell lung cancer. *N Engl J Med*. 2015;373(17):1627–1639. doi:10.1056/NEJMoa1507643
3. Etrych T, Strohalm J, Šírová M, et al. High-molecular weight star conjugates containing docetaxel with high anti-tumor activity and low systemic toxicity in vivo. *Polym Chem*. 2015;6(1):160–170. doi:10.1039/C4PY01120A
4. Hu Q, Rijcken CJ, Bansal R, et al. Complete regression of breast tumour with a single dose of docetaxel-entrapped core-cross-linked polymeric micelles. *Biomaterials*. 2015;53:370–378. doi:10.1016/j.biomaterials.2015.02.085
5. Khadka P, Ro J, Kim H, et al. Pharmaceutical particle technologies: an approach to improve drug solubility, dissolution and bioavailability. *Asian J Pharm Sci*. 2014;9(6):304–316.
6. Kang JH, Ko YT. Lipid-coated gold nanocomposites for enhanced cancer therapy. *Int J Nanomedicine*. 2015;10:33–45.

7. Su CY, Chen M, Chen LC, et al. Bispecific antibodies (anti-mPEG/anti-HER2) for active tumor targeting of docetaxel (DTX)-loaded mPEGylated nanocarriers to enhance the chemotherapeutic efficacy of HER2-overexpressing tumors. *Drug Deliv*. 2018;25(1):1066–1079. doi:10.1080/10717544.2018.1474967
8. Guo Y, Zhao S, Qiu H, et al. Shape of nanoparticles as a design parameter to improve docetaxel antitumor efficacy. *Bioconjug Chem*. 2018;29(4):1302–1311. doi:10.1021/acs.bioconjchem.8b00059
9. Khaliq NU, Park DY, Lee JY, et al. The multilayer nanoparticles for deep penetration of docetaxel into tumor parenchyma to overcome tumor microenvironment. *Colloids Surf B Biointerfaces*. 2016;146:833–840. doi:10.1016/j.colsurfb.2016.07.034
10. Marguerit G, Moustaoui H, Haddada MB, Djaker N, de la Chapelle ML, Spadavecchia J. Taxanes hybrid nanovectors: from design to physico-chemical evaluation of docetaxel and paclitaxel gold (III)-PEGylated complex nanocarriers. *Part Part Syst Char*. 2018;35(2):1700299. doi:10.1002/ppsc.v35.2
11. Jayaram DT, Ramos-Romero S, Shankar BH, et al. In vitro and in vivo demonstration of photodynamic activity and cytoplasm imaging through TPE nanoparticles. *ACS Chem Biol*. 2016;11(1):104–112. doi:10.1021/acschembio.5b00987
12. Gupta P, Singh M, Kumar R, et al. Synthesis and in vitro studies of PLGA-DTX nanoconjugate as potential drug delivery vehicle for oral cancer. *Int J Nanomedicine*. 2018;13:67–69. doi:10.2147/IJN.S177627
13. Danhier F. To exploit the tumor microenvironment: since the EPR effect fails in the clinic, what is the future of nanomedicine? *J Control Release*. 2016;244:108–121. doi:10.1016/j.jconrel.2016.11.015
14. Jain RK, Stylianopoulos T. Delivering nanomedicine to solid tumors. *Nat Rev Clin Oncol*. 2010;7(11):653–664. doi:10.1038/nrclinonc.2010.139
15. Schleich N, Danhier F, Preat V. Iron oxide-loaded nanotheranostics: major obstacles to in vivo studies and clinical translation. *J Control Release*. 2015;198:35–54. doi:10.1016/j.jconrel.2014.11.024
16. Belfiore L, Saunders DN, Ranson M, Thurecht KJ, Storm G, Vine KL. Towards clinical translation of ligand-functionalized liposomes in targeted cancer therapy: challenges and opportunities. *J Control Release*. 2018;277:1–13. doi:10.1016/j.jconrel.2018.02.040
17. Wang L, Li M, Zhang N. Folate-targeted docetaxel-lipid-based-nanosuspensions for active-targeted cancer therapy. *Int J Nanomedicine*. 2012;7:3281–3294. doi:10.2147/IJN.S30631
18. Wang L, Liu Z, Liu D, et al. Docetaxel-loaded-lipid-based-nanosuspensions (DTX-LNS): preparation, pharmacokinetics, tissue distribution and antitumor activity. *Int J Pharm*. 2011;413(1–2):194–201. doi:10.1016/j.ijpharm.2011.04.029
19. Wang TQ, Feng LX, Yang SM, et al. Ceramide lipid-based nanosuspension for enhanced delivery of docetaxel with synergistic antitumor efficiency. *Drug Deliv*. 2017;24(1):800–810. doi:10.1080/10717544.2016.1267822
20. Yan H, Wei P, Song J, et al. Enhanced anticancer activityin vitroandin vivoof luteolin incorporated into long-circulating micelles based on DSPE-PEG2000and TPGS. *J Pharm Pharmacol*. 2016;68(10):1290–1298. doi:10.1111/jphp.12598
21. Carter KA, Luo D, Razi A, et al. Sphingomyelin liposomes containing porphyrin-phospholipid for irinotecan chemophototherapy. *Theranostics*. 2016;6(13):2329–2336. doi:10.7150/thno.15701
22. Xie J, Yan C, Yan Y, et al. Multi-modal Mn–zn ferrite nanocrystals for magnetically-induced cancer targeted hyperthermia: a comparison of passive and active targeting effects. *Nanoscale*. 2016;8(38):16902–16915. doi:10.1039/C6NR03916B
23. David A. Peptide ligand-modified nanomedicines for targeting cells at the tumor microenvironment. *Adv Drug Deliv Rev*. 2017;119:120–142. doi:10.1016/j.addr.2017.05.006
24. Zhang Z, Qian H, Huang J, et al. Anti-EGFR-iRGD recombinant protein modified biomimetic nanoparticles loaded with gambogic acid to enhance targeting and antitumor ability in colorectal cancer treatment. *Int J Nanomedicine*. 2018;13:4961–4975. doi:10.2147/IJN.S177627
25. Muhamad N, Plengsuriyakarn T, Na-Bangchang K. Application of active targeting nanoparticle delivery system for chemotherapeutic drugs and traditional/herbal medicines in cancer therapy: a systematic review. *Int J Nanomedicine*. 2018;13:3921–3935. doi:10.2147/IJN.S177627
26. Xie XY, Yang YF, Yang Y, Zhang H, Li Y, Mei X. A photo-responsive peptide- and asparagine–glycine–arginine (NGR) peptide-mediated liposomal delivery system. *Drug Deliv*. 2015;23:1–12. doi:10.3109/10717544.2015.1008707
27. Dunne M, Zheng J, Rosenblat J, Jaffray DA, Allen C. APN/CD13-targeting as a strategy to alter the tumor accumulation of liposomes. *J Control Release*. 2011;154(3):298–305. doi:10.1016/j.jconrel.2011.05.022
28. Wang X, Wang Y, Chen X, Wang J, Zhang X, Zhang Q. NGR-modified micelles enhance their interaction with CD13-overexpressing tumor and endothelial cells. *J Control Release*. 2009;139(1):56–62. doi:10.1016/j.jconrel.2009.05.030
29. Negussie AH, Miller JL, Reddy G, Drake SK, Wood BJ, Dreher MR. Synthesis and in vitro evaluation of cyclic NGR peptide targeted thermally sensitive liposome. *J Control Release*. 2010;143(2):265–273. doi:10.1016/j.jconrel.2009.12.031
30. Okamoto Y, Taguchi K, Yamasaki K, Sakuragi M, Kuroda S, Otagiri M. Effect of PEGylation on the physicochemical and pharmacokinetic characteristics of bovine serum albumin-encapsulated liposome. *Asian J Pharm Sci*. 2016;11(1):112–113. doi:10.1016/j.ajps.2015.11.101
31. Riviere K, Kieler-Ferguson HM, Jerger K, et al. Anti-tumor activity of liposome encapsulated fluoroorotic acid as a single agent and in combination with liposome irinotecan. *J Control Release*. 2011;153(3):288–296. doi:10.1016/j.jconrel.2011.06.003
32. Gao LY, Liu XY, Chen CJ, et al. Core-shell type lipid/rPAA-Chol polymer hybrid nanoparticles for in vivo siRNA delivery. *Biomaterials*. 2014;35(6):2066–2078. doi:10.1016/j.biomaterials.2014.01.026
33. Lim SB, Banerjee A, Onyuksel H. Improvement of drug safety by the use of lipid-based nanocarriers. *J Control Release*. 2012;163(1):34–45. doi:10.1016/j.jconrel.2012.07.028
34. Abdus Samad Y, Sultana Y, Aqil M. Liposomal drug delivery systems: an update review. *Curr Drug Deliv*. 2007;4(4):297–305. doi:10.2174/156720107782151269
35. Pasqualini R, Koivunen E, Kain R, et al. Aminopeptidase N is a receptor for tumor-homing peptides and a target for inhibiting angiogenesis1. *Cancer Res*. 2000;60:722–727.